Journal of Biomedicine and Biosensors, 6(3):68–75, July-September: 2026.
DOI: https://doi.org/10.58613/jbb638

Journal of Biomedicine and Biosensors
ISSN (Online): 2583-3170

Journal homepage: https://www.gpub.org/journal-details.php?journal-id=45

Research Article

Semi-empirical Equation Stopping Power Calculations Electrons in Some Human Tissues

Doaa Falah Razzaq [1*]

[1] *University of Kufa, Faculty of Science, Department of Physics, Najaf, Iraq.*
[*] *Corresponding author: doaaf.aldabbag@uokufa.edu.iq*

Article Info

Keywords: *Semi-empirical, Stopping power, Electrons, Water, Blood, Skin(ICRP), Eye Lens(ICRP), Bone Cortical(ICRP) and Soft Tissue (ICRP).*

Received: *25.07.2026;*
Accepted: *12.09.2026;*
Published: *18.09.2026*

Abstract

The stopping power of electrons in the energy range of 60–260 MeV was investigated to evaluate their potential application in radiotherapy. Electron beams can be controlled electromagnetically, allowing the beam intensity to be scanned and modulated during treatment, which provides an advantage over conventional photon beams. In the present work, the stopping power of high-energy electrons was calculated for several materials relevant to radiotherapy, including water, blood, skin (ICRP), eye lens (ICRP), cortical bone (ICRP), and soft tissue (ICRP). The electron stopping power was determined using Equation (10) and the semi-empirical expression given in Equation (12). The calculated values were then compared with the corresponding results obtained from the ESTAR program. This comparison was performed over the 60–260 MeV energy range to examine the agreement between the proposed calculations and the established ESTAR data. The main purpose of this study is to provide an updated assessment of the stopping-power characteristics of electrons in materials of biological and dosimetric importance. Particular attention is given to their relevance to electron radiotherapy, where the electron beam must be accurately delivered to the target region. Finally, the semi-empirical calculations are compared with the ESTAR results to evaluate their consistency and suitability for radiotherapy-related applications. Total mass-stopping power in (MeV cm^2/g) caused by the density effect (-δ) and radiative stopping power contribution using Bragg's valence law for compound targets (Z/A) and half- 60 MeV to 260 MeV Semi-empirical stopping energy equations included in the kinetic energy T (MeV) for electrons in ranges are fitted by a three parameter approximation written using (MALAB2018) language we calculated obtained from fitting with the experimental stopping power data (ESTAR) program and we calculated the error ration STEYX and correlation coefficient. It is found that our results are in good agreement with values of Estar code and the correlation coefficient between them is (0.999).

1. Introduction

The rate of energy loss of a charged particle per unit length of the path is known as the stopping power and is written in the form (-$\frac{dT}{dx}$).

An electronic stopping ability resulting from the interaction between the incident charged particles and the electrons of the atoms, which is the subject of our current study [1].

The electronic stopping power depends on the type and energy of the charged particle as well as the properties of the material it passes through. Therefore, the ionization density along the path is related to the stopping power of the medium, while the energy loss along the path

How To Cite: D.F. Razzaq. Semi-empirical Equation Stopping Power Calculations Electrons in Some Human Tissues. *Journal of Biomedicine and Biosensors*, 6(3):68–75, 2026. https://doi.org/10.58613/jbb638

describes what happens to the charged particle. He was the first to derive the mathematical formula to calculate the stopping power of heavy particles. The charged world is the world. Bohr calculated the energy lost during the collision and found the average potential energies and distances. Bohr relied in his calculations on classical mechanics. As for Bethe, he created a formula to calculate the electronic stopping power based on quantum mechanics, and it was specific to speeds and high energies [2].

Although the topic of stopping power has been important for a century, only recently have definitive corrections to stopping power been understood and presented.

Bloch tried to understand the difference between the method of quantum mechanics and classical mechanics, and he was able to solve this contradiction when he added a correction for the electronic stopping power, which was named after him. While the even terms are neglected for higher orders of turbulence, it is also noted that collisions at a small collision dimension require scattering expansion of the Coulomb field, so what is better than the first-order Born approximation that led to the Bloch correction must be used. The main contribution to the Bloch correction appears from the transfer of small momentum and small scattering angles, including relative and non-relative velocities [3].

The study of electronic stopping power is one of the topics that has attracted the attention of researchers because of its role in the applied aspect in various fields of science such as medicine, industry and space.

Its applied importance in the field of radiotherapy is to study human tissue equivalents and determine the appropriate depth with the irradiation energy used to deliver radiation doses at different depths to the human body [4].

In this study calculated the stopping power (60-260 MeV) electrons used in radiotherapy applications in Water, Blood, Skin(ICRP), Eye Lens(ICRP), Bone Cortical(ICRP) and Soft Tissue (ICRP).

Stopping power for electrons is calculated using the Equation (10) and Semi-empirical Equation (12), then compared with experimental results obtained using the program Estar.

- Monte Carlo simulation results from the PENELOPE code have been utilized to assess the lateral spread and penetration of these beams. It has been demonstrated that the dose distribution of electron beams compares favorably with photon beams, making them a viable option for radiotherapy. Additionally, the electromagnetic control of electron beams enables scanned intensity modulation, which is not achievable with photon beams [5, 6].
- The use of very high energy electrons in radiation therapy offers several advantages. These beams can deliver a highly conformal dose to the target area while sparing surrounding healthy tissue. This precision is particularly beneficial in treating tumors located near critical organs or in pediatric patients, where minimizing radiation exposure to healthy tissue is crucial [5, 6].
- However, there are debates surrounding the implementation of very high energy electrons in radiation therapy. Some argue that the increased complexity of treatment planning and delivery may pose challenges, and the cost-effectiveness of this approach needs to be carefully evaluated. Furthermore, there is a need for further clinical studies to establish the long-term efficacy and potential side effects of using very high energy electrons in radiotherapy [5, 6].
- In conclusion, the use of electrons energy (60–260 MeV) in radiation therapy shows promise in delivering precise and effective treatment while minimizing damage to healthy tissue. However, further research and clinical trials are necessary to fully understand the implications and optimize the use of these beams in radiotherapy [5, 6].

2. Results and Discussion

2.1. Total mass stopping power of electrons

The expression for the energy loss per unit distance for the electron was obtained from the Bethe formula and can be written in the following equation.

$$\left(\frac{dT}{dx}\right)_{\text{col}} = \left(\frac{e^2}{4\pi\varepsilon_0}\right)^2 \frac{2\pi N_0\rho}{mc^2\beta^2}\frac{Z}{A}\left[\ln\left(\frac{t(t+mc^2)^2\beta^2}{2I^2mc^2}\right)+(1-\beta^2)-\left(2\sqrt{1-\beta^2}-1+\beta^2\right)\ln 2-\frac{1}{8}\left(1-\sqrt{1-\beta^2}\right)^2-\delta(x)\right]. \tag{1}$$

$$\frac{dT}{dx}_{(rad)} = \left(\frac{e^2}{4\pi\varepsilon_0}\right)^2 \frac{Z^2N_o(T+mc^2)\rho}{137m^2c^4A}\left[4\,ln\frac{2(t+mc^2)}{mc^2}-\frac{4}{3}\right] \tag{2}$$

Where $\left(\frac{dT}{dx}\right)_{\text{col}}$ and $\left(\frac{dT}{dx}\right)_{\text{rad}}$ is the collection and radiation stopping powers of electron respectively.
T is the kinetic energy of the electron.
mc^2 is the rest mass of the electron=0.511 MeV.
N is the number of atoms per in the absorber medium N= $\rho\frac{N_0}{A}$.
N_0 is the Avogadro number $6.62\times10^{-34}m^2$ kg / s.
ρ is the absorber density.
β= $\frac{v}{c}$ is the ratio of the velocity charged particle to speed of light 3×10^8 m/sec.

$\frac{Z}{A}$ are the ratio effective atomic number to atomic weight and can be find according to the Bragg's additively rule of the compound target [7–13].

$$\left\langle\frac{Z}{A}\right\rangle = \frac{\sum_j n_jZ_j}{\sum_j n_jA_j} \tag{3}$$

t = $\frac{T}{mc^2}$ is the ratio of the electron relativistic kinetic energy to its rest energy.
I is the mean excitation potential of the absorber and can be find according to the Bragg's additively rule of the compound target [14–18].

$$I \cong \begin{cases} 19.0\,\text{eV}, & Z = 1 \text{ (hydrogen)}, \\ 11.2 + 11.7Z\,\text{eV}, & 2 \leq Z \leq 13, \\ 52.8 + 8.71Z\,\text{eV}, & Z \geq 13. \end{cases} \tag{4}$$

$$ln\,\langle I \rangle = \frac{\sum_j n_j Z_j ln I_j}{\sum_j n_j Z_j} \tag{5}$$

δ(x) is the density effect correction, the numerical values of δ were fitted to the formula proposed by Stenheimer in 1952.

$$\delta(X) = \begin{cases} 4.6052X + a(X_1 - X)^M + C, & X_0 < X < X_1, \\ 4.6052X + C, & X > X_1. \end{cases} \tag{6}$$

Where,

$$X = \log(\beta\gamma) = \frac{1}{2}\log\left[(t(t+2))\right] \tag{7}$$

Where $\gamma = (1-\beta^2)^{\frac{-1}{2}}$
at $X_o <\ X$ the values of $\delta(X)$ is zero for the case of an insulator or gas, and the values of $\delta(X)$ for a metal (conductor) is small, i.e., $\delta(X) \leq 0.14$. X_1 is the value has essentially attained its asymptotic form.
a and M are adjustable parameters which will be determined below, and C is given by:

$$c = -2\,\ln\left(\frac{1}{h\nu_p}\right) - 1 \tag{8}$$

$h\nu_p$ is the plasma energy of the electron, and is given by:

$$h\nu_p = 28.816\left(\frac{\rho Z}{A}^{\frac{1}{2}} eV\right) \tag{9}$$

Where ρ is the density of medium in (g/cm^3), and (Z/A) can be find by Equation (3) [12].

The total stopping power of electrons is just the sum of the collation and radiation stopping power [14].

$$\left(\frac{dT}{dx}\right)_{tot} = \left(\frac{dT}{dx}\right)_{col} + \left(\frac{dT}{dx}\right)_{rad} \tag{10}$$

The ratio of radiation to collisional stopping powers for an electron, varies approximately [17].

$$\frac{\left(\frac{dT}{dx}\right)_{rad}}{\left(\frac{dT}{dx}\right)_{col}} \cong \frac{T}{mc^2}\frac{z}{1600} \tag{11}$$

mc^2=0.511 MeV, the energy at which this ratio is unity in MeV for the electron in the particular material.

2.2. Semi-empirical total stopping power of electrons

Semi-empirical total stopping power equations in terms of kinetic energy T (MeV) for electrons in the ranges of the low energies the high energies from 60 MeV to 260 MeV can be written as the following Equation (12).

$$\left(\frac{dT}{\rho dx}\right)_{tot} = 0.03\ T^{1.075} + 1.4, \ \ 60\ MeV \leq T \leq 260\ MeV \tag{12}$$

In actuality, the energy range (60 MeV-260 MeV) is so wide for electron beam radiation therapy, but because of it possibility use in other applications and to show compatibility of the present results with those of calculation in Equation (10) and Estar (experimental data). In addition, the values are plotted in Figures 1 - 6, for electrons in Water, Blood, Skin(ICRP), Eye Lens(ICRP) and Bone Cortical(ICRP), because of the usefulness of these results in electron beam radiation therapy.

Table 1: Density effect parameters for human blood and skin tissues (ICRP1998) [19, 20]

Tissue	Z/A	I(eV)	ρ(g/cm^3)	hν_p(eV)	-C	X_o	X_1	a	M
Water	0.55509	75	1	21.469	3.5017	0.2400	2.8004	0.09116	3.4773
Blood	0.54995	75.2	1.0600	22.001	3.4581	0.2239	2.8017	0.08492	3.5406
Skin(ICRP)	0.54932	72.7	1.1	22.400	3.3546	0.2019	2.7526	0.09459	3.4643
Eye Lens(ICRP)	0.54877	73.3	1.1	22.388	3.37	0.207	2.744	0.0969	3.455
Bone Cortical(ICRP)	0.55423	73.3	1.03	21.772	3.4279	0.2266	2.8021	0.08255	3.5585
Soft Tissue(ICRP)	0.55121	72.3	1	21.39	3.4354	0.2211	2.5728	0.08926	3.511

2.3. Total mass stopping power of electrons

When an electron enters the material, it will lose kinetic energy and constantly change direction, so after approaching the nucleus of the target atom, the electron will repeatedly recoil from its large sections of the long road. As the incident electrons are close to the surrounding electrons, there is no real interaction between them, but its interaction is similar to the interaction of equal magnetic poles. The S_{Rad} value is proportional to the incident electron energy and this situation can be interpreted as slower electrons (lower energy) electrons) spend most of their cycle time interacting with electrons and this means that these electrons have a higher chance of interacting with atomic electrons, whereas faster electrons do not it comes down to interacting with atomic electrons and passing through the Coulombic field without affecting them, thus opening up many ways for electrons to lose energy from light. Comparing the results of S_{Col} and S_{Rad}, we found that S_{Col} dominates S_{Rad} due to lower energy and hence the value of S_{tot} is significantly affected by S_{Col}.

The results of total stopping power are given in Figure 1, These results are obtained by applying Equations (1), (2), (4), (5), and (10), using the MATLAB 2018 for water and show that, on a comparative basis, the results of the semi-empirical Equation (12) agree well with the ESTAR results at STEYX (0.085) for blood, as well as correlation coefficient of 0.99. If the incident energy is in the range (60 MeV-260 MeV), it can be compared with the total energy stopping energy calculated from Equation (10), and with acceptable of STEYX (0.26) and with a of correlation coefficient (0.998) for the calculated for total stopping powers, the total mass stopping power from Equation (10) becomes has a minimum values than ESTAR results at relativistic energies because the density effect correction approaches a linear dependence on $ln(\beta\gamma)$ as in Equation (7), dependence $\left(\frac{dT}{dx}\right)_{rad}$ on the atomic number of the target and S_{tot} value depends on incident particle energy.

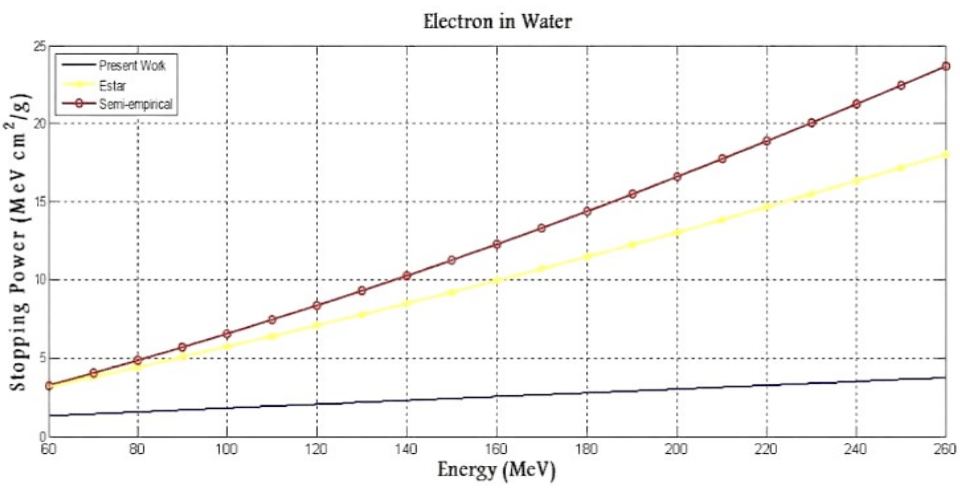

Figure 1: Show the total mass stopping power for electron at energy (60-260 MeV) in Water (ICRP) tissues obtained by present work Equation (10), Semi-empirical Equation (12) and experimental (ESTAR data)

The results of total stopping power are given in Figures 2, These results are obtained by applying (1), (2), (4), (5), and (10) using the MATLAB 2018 for Blood and show that, on a comparative basis, the results of the semi-empirical Equation (12) agree well with the ESTAR results at STEYX (0.0471) for blood, as well as correlation coefficient of 0.99. If the incident energy is in the range (60 MeV-260 MeV), it can be compared with the total energy stopping energy calculated from Equation (10), and with acceptable of STEYX (0.26) and with a of correlation coefficient (0.998) for the calculated for total stopping powers, the total mass stopping power from Equation (10) becomes has a maximum values than ESTAR results at relativistic energies because the density effect correction approaches a linear dependence on $ln(\beta\gamma)$ as in Equation (7), dependence $\left(\frac{dT}{dx}\right)_{rad}$ on the atomic number of the target and S_{tot} value depends on incident particle energy.

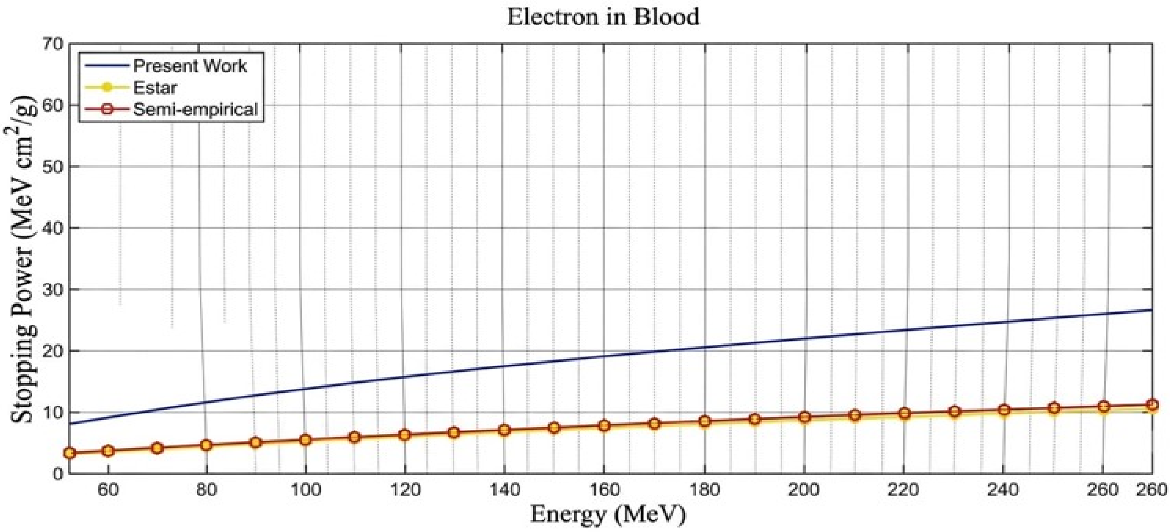

Figure 2: Show the total mass stopping power for electron at energy (60-260 MeV) in Blood (ICRP) tissues obtained by present work Equation (10), Semi-empirical Equation (12) and experimental (ESTAR data)

The results of total stopping power are given in Figures 3, These results are obtained by applying Equations (1), (2), (4), (5), and (10) using the MATLAB 2018 for Skin and show that, on a comparative basis, the results of the semi-empirical Equation (12) agree well with the ESTAR results at STEYX (0.0425) for blood, as well as correlation coefficient of 0.999. If the incident energy is in the range (80 MeV-300 MeV), it can be compared with the total energy stopping energy calculated from Equation (10), and with acceptable of STEYX (0.26) and with a of correlation coefficient (0.998) for the calculated for total stopping powers, the total mass stopping power from Equation (10) becomes has a maximum values than ESTAR results at relativistic energies because the density effect correction approaches a linear dependence on $ln(\beta\gamma)$ as in Equation (7), dependence $\left(\frac{dT}{dx}\right)_{rad}$ on the atomic number of the target and S_{tot} value depends on incident particle energy.

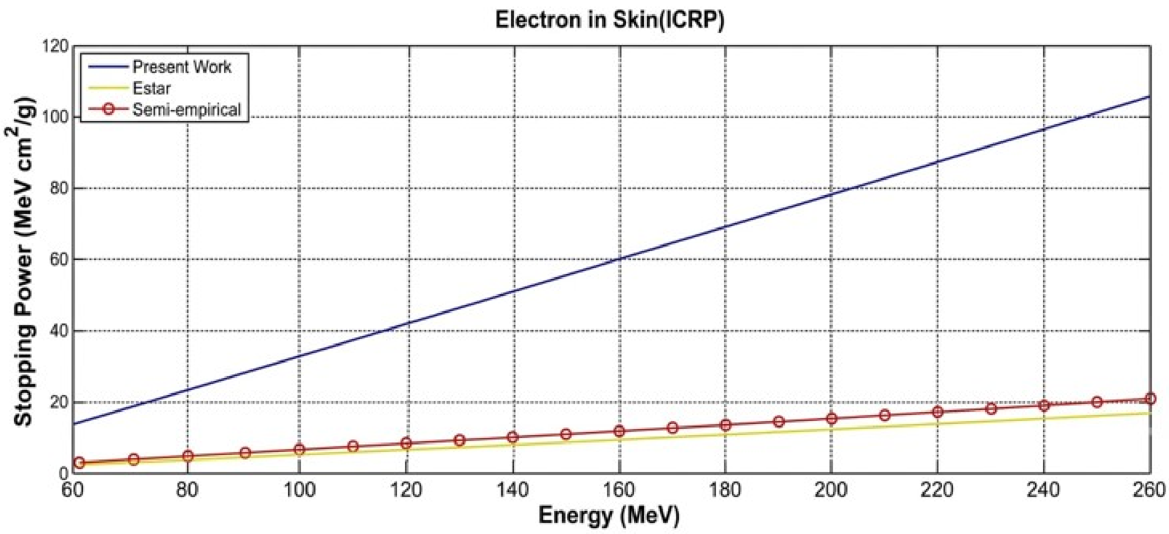

Figure 3: Show the total mass stopping power for electron at energy (60-260 MeV) in Skin (ICRP) tissues obtained by present work Equation (10), Semi-empirical Equation (12) and experimental (ESTAR data)

The results of total stopping power are given in Figures 4, These results are obtained by applying Equations (1), (2), (4), (5), and (10) using the MATLAB 2018 for Soft Tissue and show that, on a comparative basis, the results of the semi-empirical Equation (12) agree well with the ESTAR results at STEYX (0.0435) for blood, as well as correlation coefficient of 0.999. If the incident energy is in the range (60 MeV-260 MeV), it can be compared with the total energy stopping energy calculated from Equation (10), and with acceptable of STEYX (0.26) and with a of correlation coefficient (0.998) for the calculated for total stopping powers, the total mass stopping power from Equation (10) becomes has a maximum values than ESTAR results at relativistic energies because the density effect correction approaches a linear dependence on $ln(\beta\gamma)$ as in Equation (7), dependence $\left(\frac{dT}{dx}\right)_{rad}$ on the atomic number of the target and S_{tot} value depends on incident particle energy.

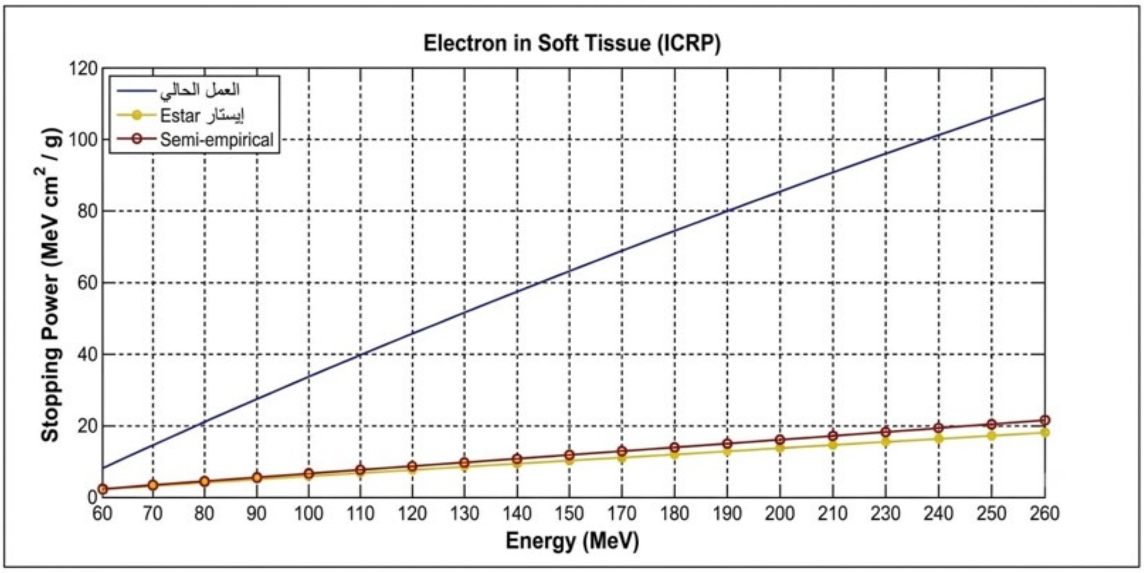

Figure 4: Show the total mass stopping power for electron at energy (60-260 MeV) in Soft Tissue (ICRP) tissues obtained by present work Equation (10), Semi-empirical Equation (12) and experimental (ESTAR data)

The results of total stopping power are given in Figure 5 and Table 1 , These results are obtained by applying Equations (1), (2), (4), (5), and (10) using the MATLAB 2018 for Bone Cortical and show that, on a comparative basis, the results of the semi-empirical Equation (12) agree well with the ESTAR results at STEYX (0.08010) for blood, as well as correlation coefficient of 0.999. If the incident energy is in the range (60 MeV-260 MeV), it can be compared with the total energy stopping energy calculated from Equation (10), and with acceptable of STEYX (0.26) and with a of correlation coefficient (0.998) for the calculated for total stopping powers, the total mass stopping power from Equation (10) becomes has a maximum values than ESTAR results at relativistic energies because the density effect correction approaches a linear dependence on $ln(\beta\gamma)$ as in Equation (7), dependence $\left(\frac{dT}{dx}\right)_{rad}$ on the atomic number of the target and S_{tot} value depends on incident particle energy.

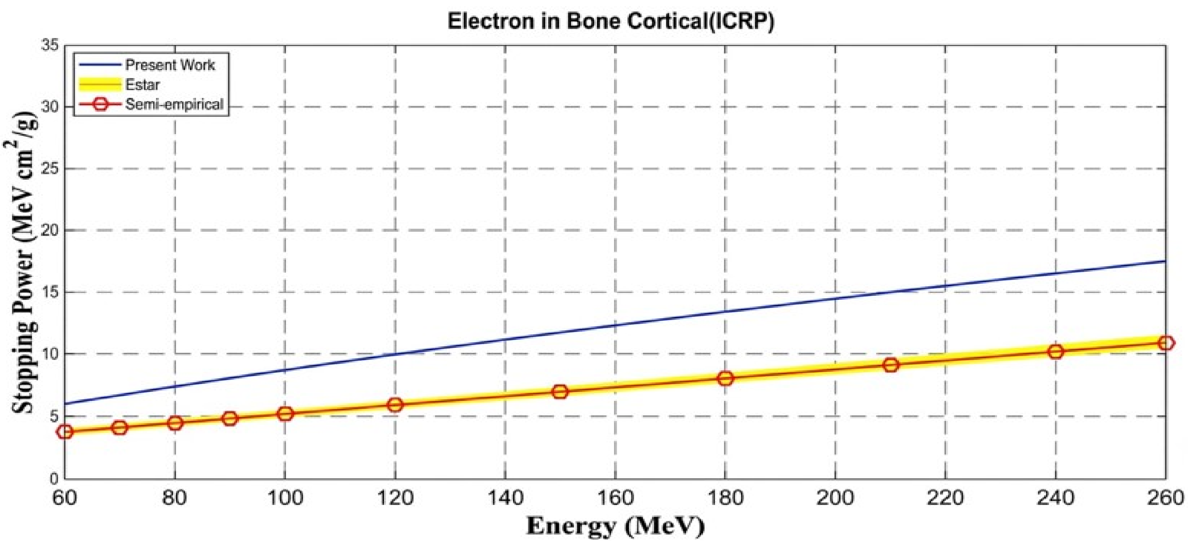

Figure 5: Show the total mass stopping power for electron at energy (60-260 MeV) in Bone Cortical (ICRP) obtained by present work Equation (10), Semi-empirical Equation (12) and experimental (ESTAR data)

The results of total stopping power are given in Figure 6, These results are obtained by applying Equations (1), (2), (4), (5), and (10) using the MATLAB 2018 for Eye Lens and show that, on a comparative basis, the results of the semi-empirical Equation (12) agree well with the ESTAR results at STEYX (0.0424) for blood, as well as correlation coefficient of 0.999. If the incident energy is in the range (60 MeV-260 MeV), it can be compared with the total energy stopping energy calculated from Equation (10), and with acceptable of STEYX (0.26) and with a of correlation coefficient (0.998) for the calculated for total stopping powers, the total mass stopping power from Equation (10) becomes has a minimum values than ESTAR results at relativistic energies because the density effect correction approaches a linear dependence on $ln(\beta\gamma)$ as in Equation (7), dependence $\left(\frac{dT}{dx}\right)_{rad}$ on the atomic number of the target and S_{tot} value depends on incident particle energy.

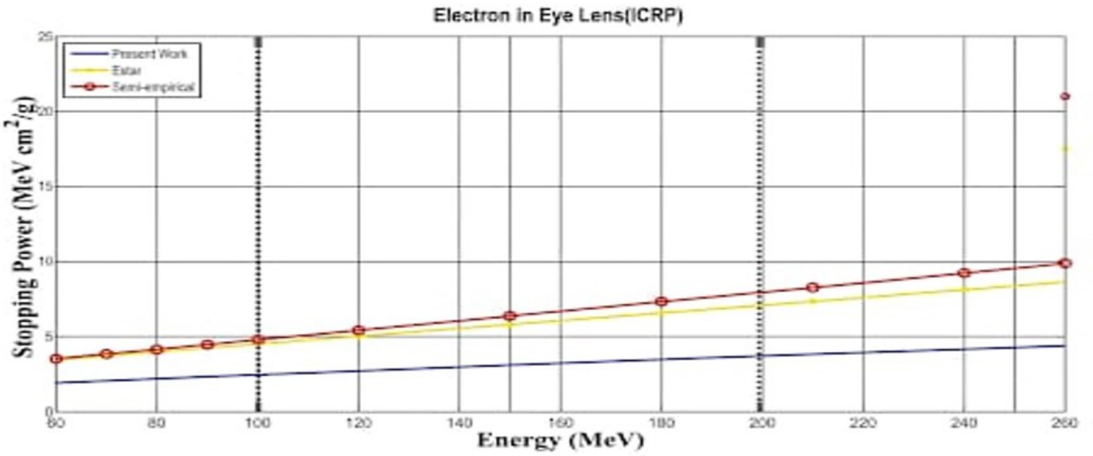

Figure 6: Show the total mass stopping power for electron at energy (60-260 MeV) in Eye Lens (ICRP) tissues obtained by present work Equation (10), Semi-empirical Equation (12) and experimental (ESTAR data)

3. Conclusions

It is clear from the results obtained with the proposed semi-empirical Equation (12) applied to electron emission in Water, Blood, Skin(ICRP), Eye Lens(ICRP) and Bone Cortical(ICRP) and Soft Tissues(ICRP) that the total mass stopping power of electron in this materials can be expressed in terms of energy. It is also worth mentioning that the proposed Semi-empirical equation is simpler, more applicable and the results are in better agreement with the experimental (ESTAR data) compared to the results of Equation (10). The presented tables are expected to be helpful in quantitative planning in electronic therapy , since the tables mainly contain the number of electronic interactions and moreover, the proposed method is easily applicable to new targets , composite or not. It should be noted that the method proposed here can only be applied projectively with electrons and positrons. Statistics show that the S_{tot} decreases with increasing particle penetration energy, and this energy depends on the particle velocity that limits the type of interaction with the target. The Stot value depends on the energy of the incident particle and the atomic number of the target. It was observed the difference was significant between results obtained from Equation (10) and ESTAR when the energy (60-260 MeV). That is, the Bethe-Bloch equation need to be corrected.

Article Information

Funding: The authors received no external funding for this study.

Ethical Approval: Ethics committee/IRB approval was not applicable to this study, as it involved theoretical and computational calculations only.

Informed Consent: Informed consent was not applicable to this study, as it was a theoretical and computational study and did not involve human participants.

Conflict of Interest: The authors declare no competing interests.

Data Availability Statement: The data generated and/or analyzed during this study are available from the corresponding author upon reasonable request.

Acknowledgments: The authors would like to express their sincere gratitude to Prof. Dr. Ahmed Abdul-Jabbar for his valuable assistance and support during this research.

Disclaimer (Artificial Intelligence): The author(s) hereby declare that NO generative AI technologies such as Large Language Models (ChatGPT, COPILOT, etc.), and text-to-image generators have been used during writing or editing of manuscripts.

References

[1] J. F. Ziegler, J. P. Biersack, and U. Littmark. *The stopping and range of ions in solids*. Pergamon Press, New York, 1985.

[2] A Getachew. Stopping power and range of protons of various energies in different materials. Master's thesis, Addis ababa University, 2007.

[3] R. Lozeva. *A new developed calorimeter telescope for identification of relativistic heavy ion reaction channels*. PhD thesis, University of Sofia, Sofia, Bulgaria, 2005.

[4] M. S. Khalifa, S. F. Aloraby, and N. A. Shahbon. Use of plastic detectors (CR-39) for characterization of the linear energy transfer (LET) of -particles in air. In *Ninth arab conference on the peaceful uses of atomic energy, Beirut*, Beirut, Lebanon, 2008.

[5] L. Papiez, C. DesRosiers, and V. Moskvin. Very high energy electrons (50–250 MeV) and radiation therapy. *Technology in cancer research & treatment*, 1(2):105–110, 2002. URL `https://doi.org/10.1177/153303460200100202`.

[6] M.G. Ronga, M. Cavallone, A. Patriarca, A.M. Leite, P. Loap, V. Favaudon, G. Créhange, and L Marzi. Back to the Future: Very High-Energy Electrons (VHEEs) and Their Potential Application in Radiation Therapy. *Cancers*, 13(19):4942, 2021. URL https://doi.org/10.3390/cancers13194942.

[7] H. S. Hadi and R. O. Kadhim. Stopping power calculations of electron in six types of human tissue for energies (20–20000 ev). *Journal of Kufa-Physics*, 9:23–35, 2017.

[8] R. O. Kadhim and S. J. Abdulrazzak. Calculation of the Electronic Stopping Power of Hydrogen Ions in Some Tissues of the Human Body. *Biochem. Cell. Arch.*, 18(1):703–707, 2018.

[9] T. A. J. Younis and F. M. Hady. Calculation of The Stopping Power of Alpha Particles and Its Range in Bone Tissue. *International Journal of Research Granthaalayah*, pages 315–320, 2019.

[10] M. J. Berger and S. M. Seltzer. *Stopping powers and ranges of electrons and positrons*. National Bureau of Standards, 1982. URL https://doi.org/10.6028/NBS.IR.82-2550.

[11] M. O. El-Ghossain. Calculations Of Stopping power, and range of electrons interaction with different material and human body parts. *International journal Of scientific and technology research*, 1:114–115, 2017.

[12] M.J. Gazda and L.R. Coia. Principles of radiation therapy. *Cancer network*, pages 9–19, 2001.

[13] K. S. Krane. *Introductor nuclear physics*. John Wiley & Sons, 1987.

[14] P. G. Rancoita and C. Leroy. *Principles of radiation interaction in matter and detection, University de montreal*. World Scientific, 2 edition, 2009.

[15] J. F. Ziegler. The stopping of energetic light ions in elemental matter. *J. Appl. Phys / Rev. Appl. Phys.*, page 6, 1999.

[16] N. Tsoulfanidis. *Measurement and detection of radiation*. University of missouri-rolla, second edition, 1995. Pages 262-246.

[17] G. Tanır, M. H. Bölükdemir, S. Keleş, and I. Göker. On the stopping power for low energy positrons. *Chinese journal of physics*, page 426, 2011.

[18] M. O. El-Ghossain. Calculations Of Stopping power, and range of electrons interaction with different material and human body parts. *International journal Of scientific and technology research*, 1:114–115, 2017.

[19] R. S. Detwiler, R. J. McConn, T. F. Grimes, S. A. Upton, and E. J. Engel. Compendium of material composition data for radiation transport modeling. Technical report, Pacific Northwest National Laboratory, 2011.

[20] D. F. Razzaq, M. R. Taher, and A. A. Abojassim. Estimation of stopping power of high energy electrons in eye lens, bone cortical and soft tissue. *International Journal of Physics and Applications*, 7(1):259–265, 2025.